Journal of Electrical Engineering, Vol. 76, No. 2, 2025, pp. 175-183

Interpolation-based optimal s-to-z mapping functions for IIR design

Shalabh K. Mishra[1], Om Prakash Goswami[2], Nawnit Kumar[3], Aasheesh Shukla[4]

In this paper, novel low-order s-to-z mapping functions are proposed. The methodology employs an interpolation framework that combines the first-order bilinear transform and the Adams-Moulton numerical integration formula, utilizing distinct interpolating variables. The resulting transfer functions effectively map the s-plane to the z-plane, achieving an accurate approximation of the ideal magnitude and phase response in the transition from the analog to the digital domain. Notably, the relationship between the analog frequency (Ω) and the discrete frequency (ω) exhibits maximal linearity over an extended frequency range, rendering the proposed approach highly suitable for infinite impulse response (IIR) filter design. Furthermore, the derived mapping functions are applied in the design of digital low-pass filters for various quality factor values. Simulation results demonstrate a significant enhancement in the frequency response within the digital domain compared to existing mapping techniques. Additionally, experimental validation is conducted using a Simulink-based design model, confirming the efficacy of the proposed approach.

Keywords: aliasing, IIR filters, bilinear transformation, fractional-order filters, s-to-z mapping, warping effect

1 Introduction

Electronic filters are the key components in communication systems and play a vital role in signal selection, noise reduction, and system performance improvement. There are several types of filters based on their pass-band and stop-band behavior, such as low-pass, high-pass, band-pass, all-pass, band-reject, comb filter, etc. [1-4]. Filters can be categorized as analog filters and digital filters, both of which have their own merits and limitations. Unlike analog filters, digital filters are composed of delays, multipliers, and adder circuits in place of resistors, inductors, and capacitors [5,6]. Digital filters have some important merits over their analog counterparts, such as superior performance-to-cost ratio, system flexibility, programmability, and resistance to manufacturing variations, temperature, humidity, and aging. There are two design topologies named IIR (infinite impulse response) and FIR (finite impulse response) utilized in digital filter designing. Both techniques have their own advantages and disadvantages but IIR-based designs contribute less memory requirement and computational time as compared to FIR. Therefore, due to the wide area of applications in control theory, speech processing, radar, telecommunication systems, and biomedical signal processing, researchers have always had a great interest in the area of filter designing using the IIR technique. In conventional IIR filter designing, filters with the desired specifications are designed in the analog domain first, and then transferred into the digital domain using appropriate analog-to-digital (s-to-z) mapping functions. Several s-to-z mapping functions are available in the literature [7-11], such as bilinear, Al-Alaoui, Schneider, etc. Bilinear transformation provides the first-order s-to-z mapping function and is widely used in IIR designing. The bilinear transformation does not produce linear s-to-z mapping, consequently, the digitally transferred systems suffer from frequency warping and fail to replicate the analog system into its digital counterpart. Although, to counter this warping effect frequency pre-warping could be done, several limitations of the pre-warping have also been reported [12-14]. In addition to the first-order bilinear transform, higher-order s-to-z mapping functions have also been developed using numerical integration techniques [12, 15-17]. These higher-order mapping functions have been used in the designing of IIR filters since they may have acceptable linearity compared to the lower-order mapping functions [12-14].

Additionally, numerous attempts have been made to combine and interpolate different techniques to propose improved methodologies. Al-Alaoui [11] observed that the ideal digital integrator's (DI) magnitude response lies between the responses of the rectangular and trapezoidal integration rules. Consequently, interpolating between these two rules offers a new approximation of the ideal integrator, leading to the design of a digital differentiator (DD) with appropriate modifications. In [18], a prominent method involves applying the Z-transform to the Newton-Cotes integration formula, which led to the development of a new third-order wideband trapezoidal digital integrator. This integrator stands out for its precision in approximating an ideal integrator over the Nyquist frequency range. Another line of research

[1]Electronics and Communication Engineering Department, Thapar Institute of Engineering and Technology, Punjab, India
[2]KJ Somaiya School of Engineering, Somaiya Vidyavihar University, Mumbai, India
[3]Sri Guru Tegh Bahadur Institute of Management & IT, New Delhi, India
[4]Department of Electronics & Communication, GLA University, Mathura, India
shalabh.mishra@thapar.edu,

https://doi.org/10.2478/jee-2025-0018, Print (till 2015) ISSN 1335-3632, On-line ISSN 1339-309X

explores enhancing the accuracy of digital integrators through trapezoidal integration, differential equations, and Richardson extrapolation [19]. This approach integrates a Lagrange finite-impulse response (FIR) fractional delay filter to optimize the performance of the digital integrator, offering both accuracy and efficiency. Additionally, the use of the discrete Hartley transform (DHT) in combination with numerical integration rules has resulted in a closed-form solution for digital integrators [20]. This approach simplifies the computation of filter coefficients and improves the performance when compared to traditional integrators. Cadan [21], employed numerical interpolation methods to approximate both the magnitude and phase of the ideal integrator with low-order designs being particularly relevant for applications such as strap-down inertial navigation. Additionally, a weighted interpolation approach between Boole's rule, the trapezoidal rule, and Simpson's rule was explored to produce a third-order transfer function that closely approximates the ideal differentiator [22]. Furthermore, several other designs have been proposed based on interpolation techniques that utilize a variable weighting factor [10, 23]. Recently, efforts have also targeted optimizing IIR digital differentiators of the first and second orders using fractional interpolation of bilinear and rectangular transforms [24]. All of these designs, based on various interpolation methods and mathematical formulations, represent significant advancements in the development of digital differentiators. However, for differentiators used in IIR filter design, it is crucial to match both phase accuracy and magnitude.

Apart from all this, various approximation-based operators and nature-inspired metaheuristic optimization algorithms have also been utilized to transform the analog domain into the digital domain [25-31]. However, a serious attention is paid only to the precise magnitude mapping while completely ignoring the phase correlation for the approximation of digital differentiator. Therefore, it is observed that an s-to-z transform’s accurate approximation may be used as the digital differentiator, but vice-versa may not be true. Therefore, in this work, an attempt is made to develop a more accurate s-to-z mapping function for IIR filter designing.

The organization of the paper is as follows. Section 2 discusses the various types of available s-to-z mapping functions and their characteristics. This section also discusses the suitability of the s-to-z mapping function for designing of IIR filter. A new 3rd-order s-to-z mapping function is proposed in section 3, by using the interpolation of first-order Bilinear transform and 3rd-order Schneider transform. In section 4, IIR filters have been designed and simulated by transforming an existing analog filter into a digital domain, by using existing and proposed s-to-z mapping function. Further, a thorough comparison of these designed IIR filters has been done in this section, to analyze the performances of discussed s-to-z mapping functions. Finally, conclusions are given in Section 5.

2 Mapping of Analog to Digital Domain

There are several well-known s-to-z mapping schemes derived from logarithmic expansion (bilinear transform), Adams-Moulton numerical integration formulas [13, 17]. The corresponding mapping functions are summarized in Table 1.

Table 1. s-to-z mapping functions

Transformation	Mapping Function
1st -order Bilinear [11, 16]	$\frac{2(z-1)}{T(z+1)}$
2nd -order Schneider [13, 15, 16]	$\frac{12(z^2-z)}{T(5z^2+8z-1)}$
3rd-order Schneider [13, 15, 16]	$\frac{24(z^3-z^2)}{T(9z^3+19z^2-5z+1)}$
4th -order Schneider [13, 15]	$\frac{720(z^4-z^3)}{T\left(\begin{array}{l}251z^4+646z^3-\\264z^2+106z-19\end{array}\right)}$
5th-order Schneider [13, 15]	$\frac{1440(z^5-z^4)}{T\left(\begin{array}{l}476z^5+1427z^4-798z^3\\+482z^2-173z+27\end{array}\right)}$

The magnitude and phase mapping of the s-plane to the z-plane for the above transformations are shown in Fig. 1. It is observed that 1st-order bilinear transformation provides accurate phase mapping but is unable to maintain acceptable magnitude mapping beyond 0.95 radians. The 2nd-order Schneider operator is capable of providing accurate magnitude mapping beyond 1 rad/sec but fails to maintain accurate phase mapping throughout the Nyquist frequency range.

Similarly, other higher-order mapping functions (3rd order, 4th order, and 5th order) give accurate magnitude and phase mapping up to a certain frequency band. Though the frequency bandwidth of this mapping varies with the change of its order, but as the order increases, a greater number of poles-zeros are added to the system which may affect the stability of the systems. Additionally, these extra poles and zeros increase the cost and complexity of the system. Therefore, lower-order mapping functions are often preferred over higher-order functions if the s-to-z mapping characteristic doesn’t affect significantly. From Fig. 1, it is also noticeable that the 1st order bilinear transformation gives accurate phase mapping in the complete frequency band whereas the 3rd order transformation (Schneider) gives satisfactory magnitude mapping. Although, these two mapping functions don't provide adequate magnitude as well as phase mapping simultaneously. Therefore, an attempt is made to develop a new s-to-z mapping function by interpolating these two mapping functions, which can provide magnitude as well as phase mapping up to a greater band.

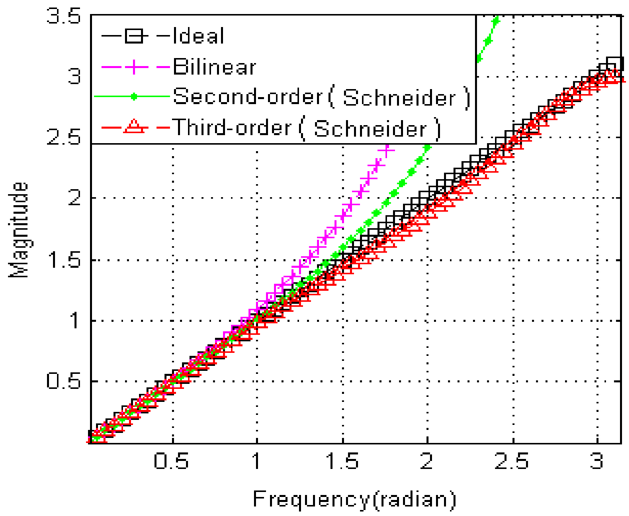

(a)

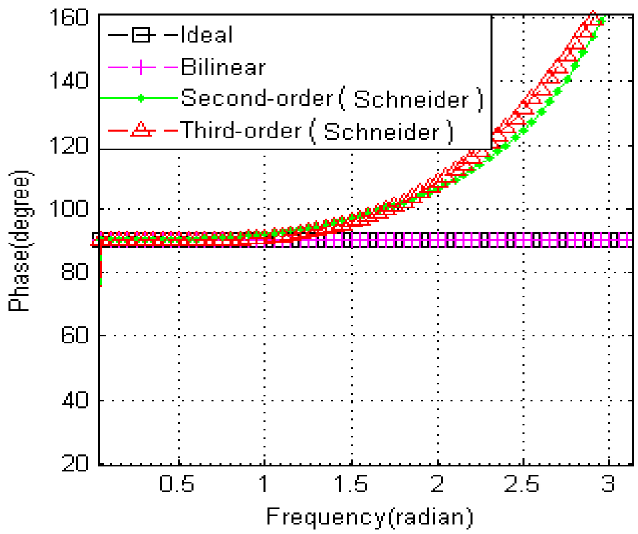

(b)

Fig. 1. Magnitude and phase mapping of existing s-to-z transform

3 Proposed s-to-z mapping function

As discussed in the previous section, the 1st-order bilinear transformation gives accurate phase mapping but is unable to provide satisfactory magnitude mapping whereas the 3rd-order transformation gives acceptable magnitude mapping but fails to maintain adequate phase mapping. This observation gives an intuition that s-to-z mapping can be deduced by combining the 1st and 3rd-order mapping functions to provide a trade-off balance between phase and magnitude mapping, and could be used for IIR filter designing. Therefore, an interpolation between 1st-order bilinear transformation and 3rd-order transformation can be written as

$$H(Z) = \alpha\frac{2(Z-1)}{T(Z+1)} + (1-\alpha)\frac{24(Z^3-Z^2)}{T(9Z^3+19Z^2-5Z+1)} \tag{1}$$

where α is the weightage factor (lesser than unity), and T is the sampling period. The sampling period affects accuracy, stability, and computational efficiency. It influences frequency warping, where improper selection distorts the frequency response. A smaller T improves accuracy but increases computational complexity, while a larger T may degrade system approximation. Proper choice of T ensures stability, prevents aliasing, and balances performance in digital signal processing and control systems. Often, T=1 is chosen for mathematical simplicity and normalization, simplifying transformations by removing explicit dependence on T. This makes computations easier and allows for a standardized discrete-time analysis.

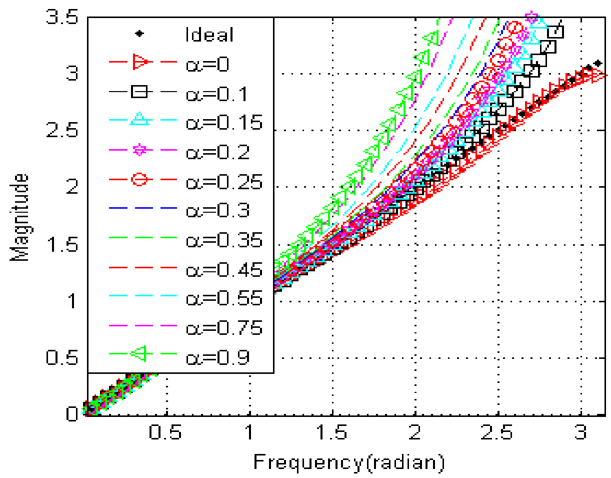

(a)

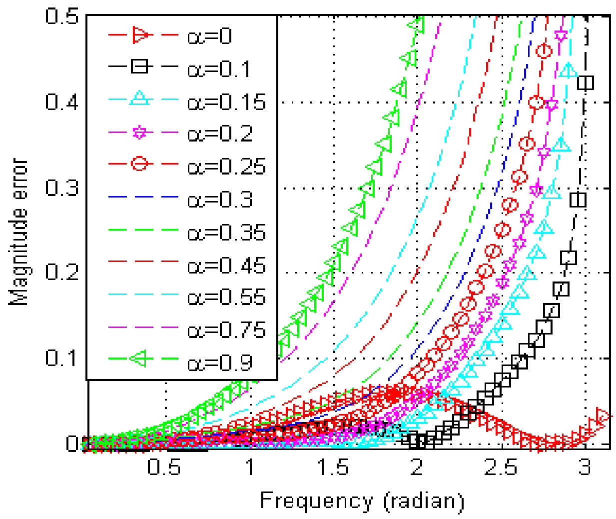

(b)

Fig. 2. Magnitude response and corresponding error of proposed interpolations

The magnitude and phase response of the proposed interpolated mapping function is obtained assigning appropriate values of α. The magnitude response and phase response with the corresponding error plots are shown in Figs. 2 and 3 respectively. The results observed from the proposed mapping function reveal that it delivers significant and reliable outcomes when the value of α is in the range of 0.15 to 0.25. The proposed mapping function, which consists of 75% to 85% third-order characteristics and 15% to 25% bilinear character-ristics, generates accurate and well-justified magnitude and phase mappings. This balance between third-order and bilinear characteristics is critical, as it ensures that the magnitude and phase mapping produced by the function are both accurate and well-justified. As a result, the interpolation values corresponding to α = 0.15, 0.2, and 0.25 are chosen for further processing due to their optimal performance in generating precise mappings. The magnitude and phase responses of these selected interpolations are compared with several other existing well-known and higher-order mapping functions illustrated in Fig. 4.

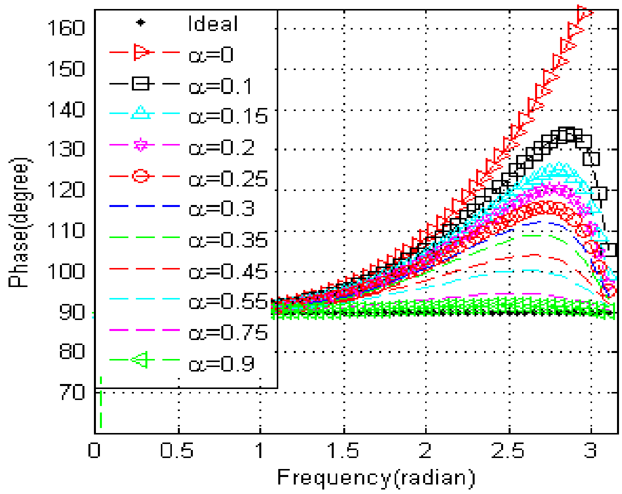

(a)

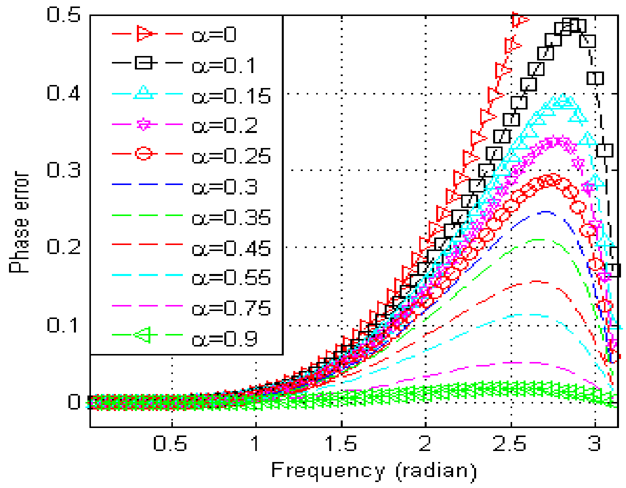

(b)

Fig. 3. Phase response and phase error of proposed interpolations

It can be visualized that the proposed mapping functions give satisfactory magnitude and phase resemblance with the ideal one. Thus, the proposed design may act as an optimal s-to-z mapping function for IIR designing. Fig. 5 further confirms the linear mapping between analog frequency (Ω) and discrete frequency (ω).

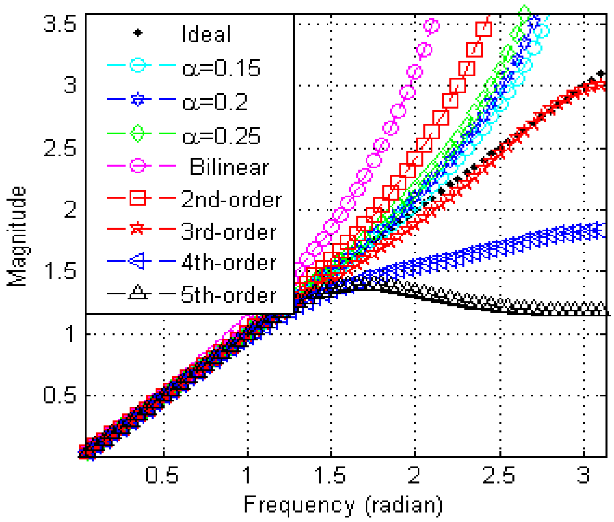

(a)

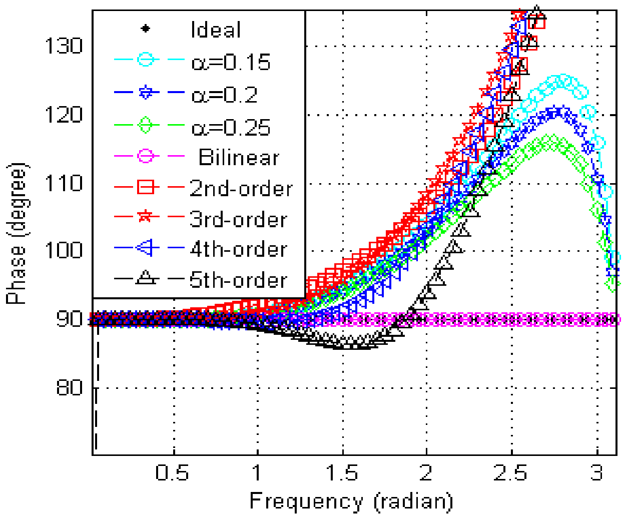

(b)

Fig. 4. Comparisons of (a) magnitude and (b) phase response of the proposed interpolations with the existing mapping functions.

An optimal mapping function should have perfect linearity and maximum span for the analog frequency versus the digital frequency [13-14]. It is observed that the bilinear transformation can retain the linearity up to 0.95 radian only, whereas this linearity extends up to 1.2 to 1.4 radian for the existing 2nd order 3rd order 4th order and 5th order mapping functions. It is interesting to visualize that the proposed mapping functions show maximum linearity, i.e., more than 1.5 radian. Thus, the proposed 3rd-order mapping functions are capable of maintaining higher linearity and wider frequency span than the existing higher-order (4th and 5th order) mapping functions also. Since these 3rd-order mapping functions have fewer numbers of poles and zeros, the proposed 3rd-order mapping functions are certainly preferable over the existing higher-order mapping functions for IIR realizations. Moreover, the proposed transforms are free from aliasing as they map the entire s-plane (-∞ to +∞) to z-plane (-π to +π) with maximum linearity.

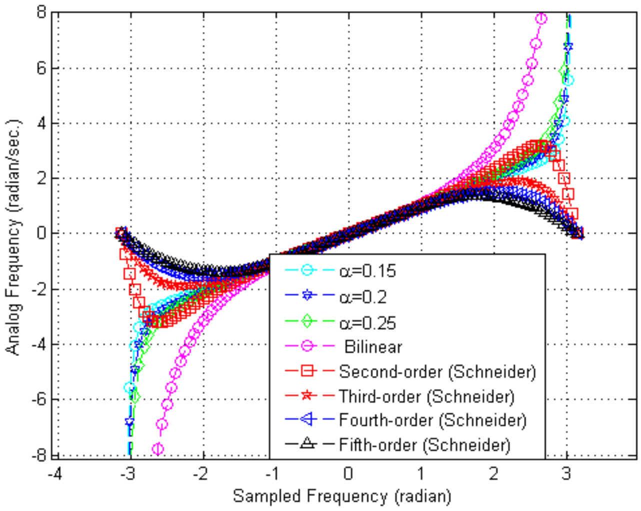

Fig. 5. Mapping of analog vs. discrete frequency

4 Design validation

To analyze the appropriateness of the proposed mapping functions, existing pre-specified analog filters are considered for IIR designing. The generalized transfer function of the considered system is [32]:

$$H(s)=\frac{\omega_c^2}{s^2+(\omega_c/Q)s+\omega_c^2} \tag{2}$$

where Q is the quality factor and ω_c is the cut-off frequency in rad/sec. The cut-off frequency and sampling period are taken as 1 rad/second and 1 second, respectively, to satisfy the minimum Nyquist sampling criterion. This filter is discretized by the proposed and some existing s-to-z mapping functions for several different quality factors as: 0.5, 1, 4, and 10 respectively. The corresponding magnitude response and the relative error in gain are shown in Figs. 6, 7, 8, and 9. The peak relative error within the –20 dB passband, and the sum of relative errors up to 2 rad/sec., are listed in Tab. 2.

It is observed that the peak relative error and the cumulative error for the considered IIR filter designed using the 1st-order Bilinear transformation are ranging from 0.19 to 0.8 and from 6.4 to 13.2, respectively. Similarly, the same errors for the 2nd-order Schneider operator-based design are ranging from 0.4 to 1.8 and from 0.8 to 7, respectively. Further, the peak relative error and the cumulative error for the 3rd, 4th, and 5th order mapping function-based design are increased up to 2.5 and 15.5 respectively. However, the proposed mapping function shows the peak relative error and the cumulative error of 0.6 and 2.5 respectively, even in the worst cases.

Therefore, the proposed 3rd order interpolation-based mapping function gives significantly improved results than the existing mapping functions. This observation can also be validated by analyzing the cumulative errors for the proposed and existing mapping functions summarized in Tab. 2. Additionally, it is also noticed that the $\alpha=0.25$ based interpolation gives better results than the $\alpha=0.2$ and $\alpha=0.15$ based interpolations for the low-quality factor, i.e., Q=0.5 and Q=1; however, the $\alpha=0.15$ based interpolation gives better result than $\alpha=0.20$ and $\alpha=0.25$ based interpolations for the high-quality factor, i.e., Q = 4 and 10. Therefore, it is suggested that for high-quality filters interpolation with the lower value of α should be preferred over the higher α and vice versa.

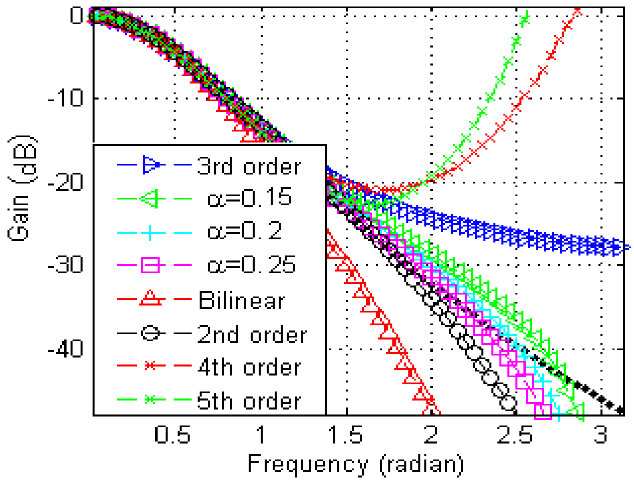

(a)

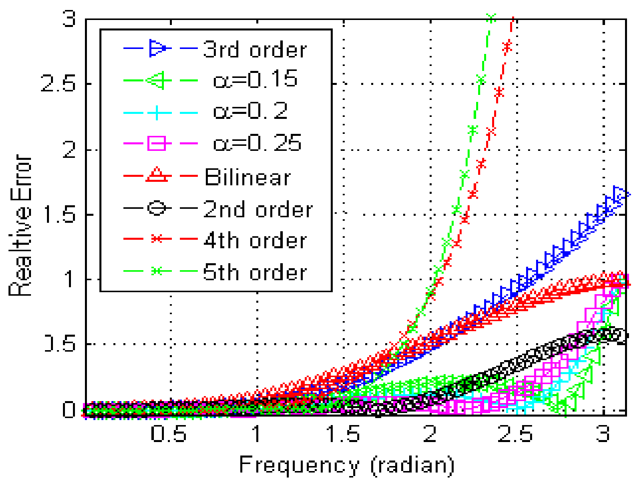

(b)

Fig. 6. Magnitude response and gain error for Q= 0.5

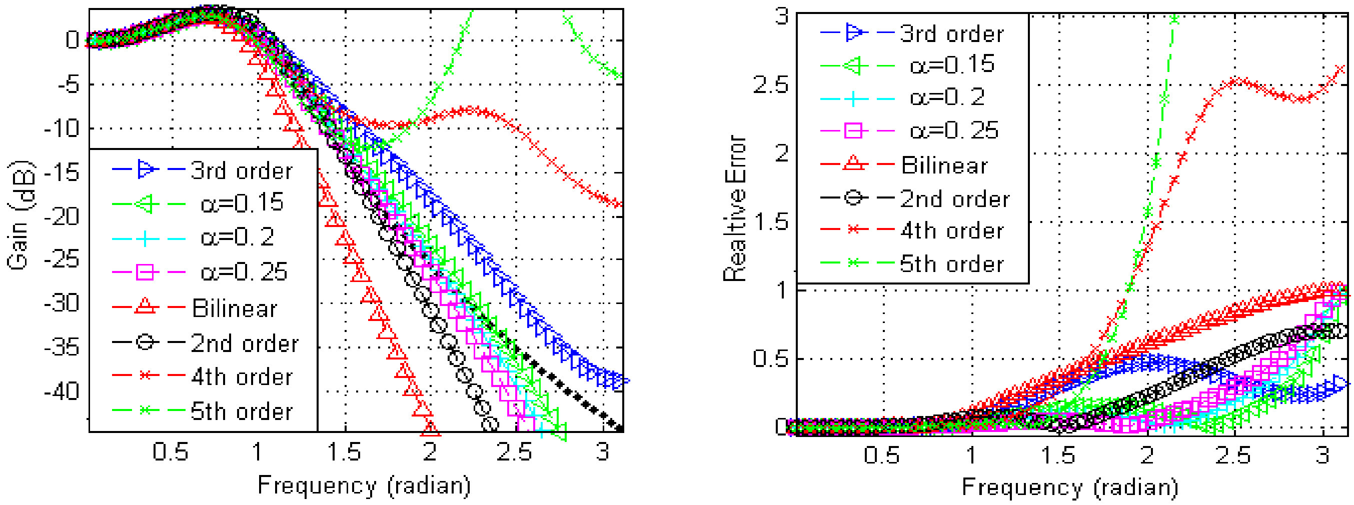

Fig. 7. Magnitude response and gain error for Q = 1

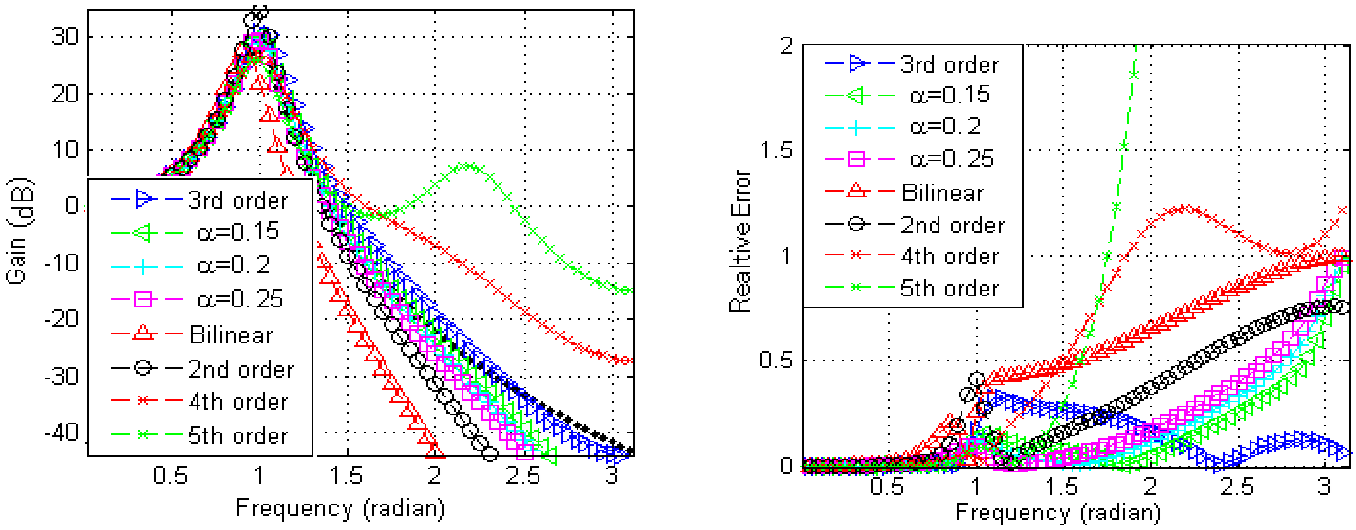

Fig. 8. Magnitude response and gain error for Q = 4

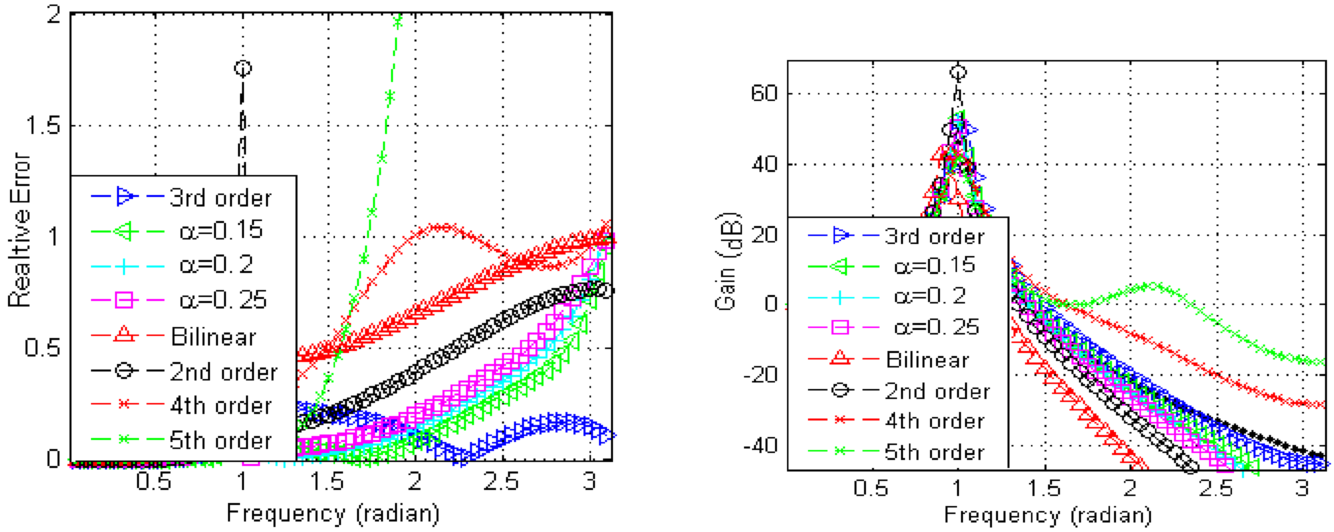

Fig. 9. Magnitude response and gain error for Q = 10

Table 2. Peak and cumulative magnitude error for the designed IIR filters

Transformation		Peak relative error within –20 dB band				Cumulative error (up to 2 rad/sec) with sampling interval 0.05 rad/sec			
		Q=0.5	Q=1	Q=4	Q=10	Q=0.5	Q=1	Q=4	Q=10
Bilinear		0.19	0.5	0.63	0.8	6.4	7.9	11.2	13.5
2nd-order (Schneider)		0.04	0.1	0.42	1.8	0.8	2	5	7
3rd-order (Schneider)		0.11	0.3	0.32	0.85	4.6	5.9	5.2	5.5
4th-order (Schneider)		0.08	0.7	1.1	1	5.7	8.8	11.5	11.9
5th-order (Schneider)		0.02	0.58	2.3	2.5	4.5	7.4	14.2	15.5
Proposed 3rd order	$\alpha = 0.25$	0.05	0.15	0.34	0.6	0.7	0.6	1.7	2.5
	$\alpha = 0.2$	0.1	0.12	0.36	0.4	1.2	1.5	1.3	1.7
	$\alpha = 0.15$	0.15	0.15	0.4	0.3	2.1	2.4	1.7	1.6

Further, the Simulink model is used for experimental validation of the accuracy of the proposed design methodology. The Simulink model of this arrangement is shown in Fig. 10. This experimental setup was done for the low pass filter of unit quality factor and normalized cutoff frequency.

In this simulation, a sinusoidal waveform of 1.257 rad/sec (sampled with time-period T=1sec.) is taken as an input signal and passed through the IIR filters designed using a few optimal s-to-z mapping functions. After passing through the IIR filters, signals are passed through the analog low-pass filter to convert the sampled signal into a continuous-time signal. Further, all these signals are multiplexed and connected to a display. These responses are also compared with the ideal filter response as illustrated in Fig. 11.

It can be observed that the peak amplitude of the sinusoidal signal drops to 0.5 V from 1 V after passing through the 1st-order Bilinear transform-based IIR filter. This attenuation improves slightly up to 0.5 V for the 2nd-order transform-based IIR filter, whereas the peak amplitude of the 3rd-order transform-based IIR filter shoots abruptly up to 1.8 V, which is almost twice the expected outcome. The peak amplitude of the proposed interpolation-based IIR design is 0.9 V which is quite close to the ideal response. Thus, the proposed interpolation-based s-to-z operator (with $\alpha = 0.2$) is capable of replicating the ideal response with minor attenuation whereas the responses of other existing operator-based designs deviate significantly from the ideal response.

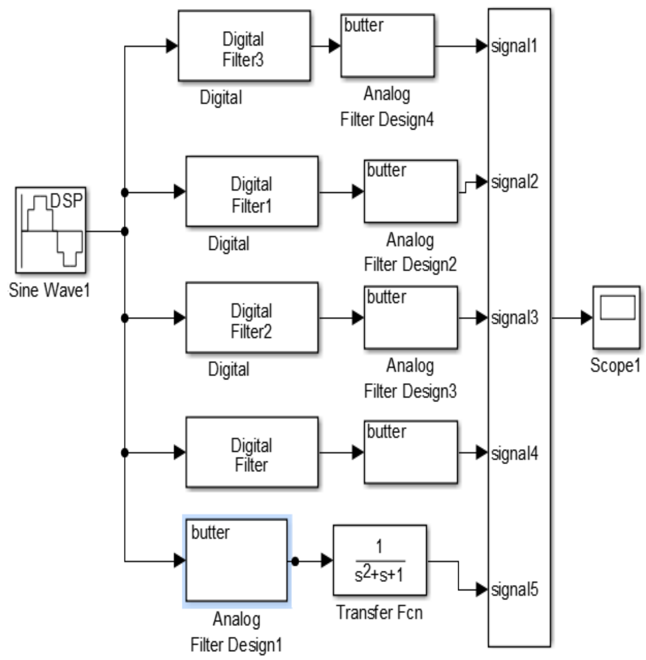

Fig. 10. Simulink design model of the IIR filters

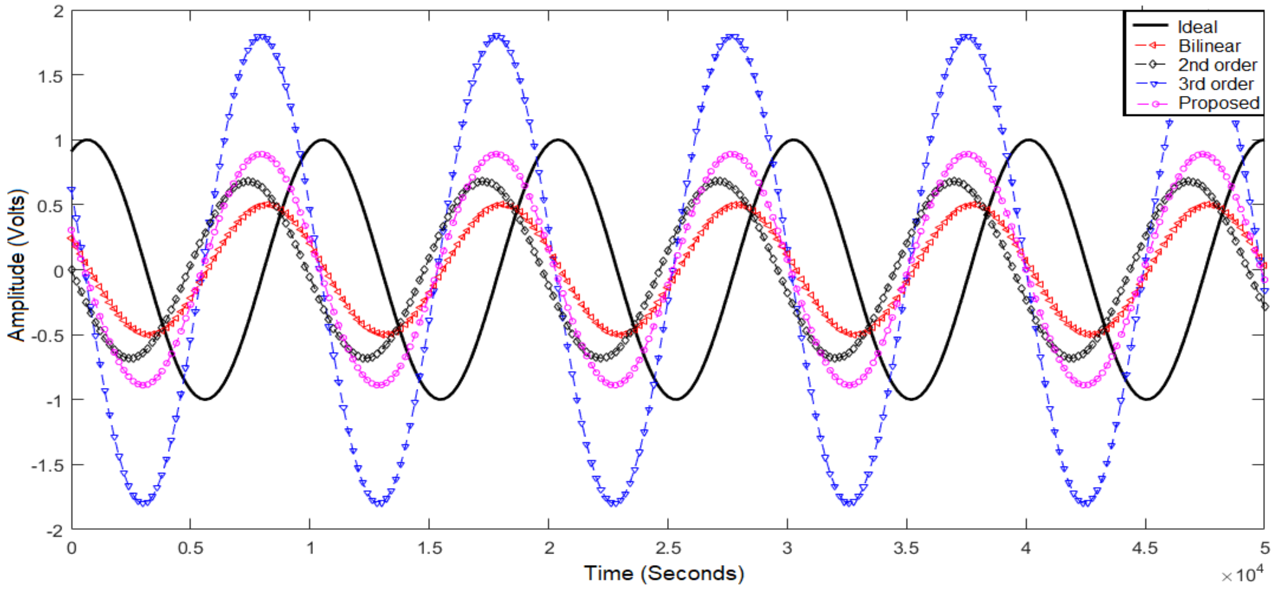

Fig. 11. Simulink response of the IIR filters for the sinusoidal input

5 Conclusion

This study has introduced efficient s-to-z mapping functions based on the interpolation of the first-order bilinear transform and the third-order Schneider transformation. The proposed mapping functions achieve an optimal mapping of the s-plane to the z-plane, ensuring the widest frequency span with maximal linearity. Consequently, these functions are well-suited for the design of infinite impulse response IIR filters.

The efficacy of the proposed approach is further validated through the design of digital low-pass filters for various quality factor values. It is observed that the Peak Relative Error (within –20 dB band) ranges from 0.05 to 0.6 for the proposed techniques whereas this range expand upto 0.85 for the existing design of the same order. Similarly, the Cumulative Error (up to 2 rad/sec) for the existing 3rd and 4th order design is up to 11.9 whereas for the proposed design it reduces to 2.9. The results confirm a superior approximation of the analog filter response compared to existing mapping techniques. Further, the experimental validation with a Simulink-based model confirms the simulation results, showing the design's practical viability. The passband sinusoidal signal processed through IIR filters retains its peak amplitude with minimal distortion, while conventional methods cause significant changes in the passband signal.

Therefore, the proposed low-order wideband s-to-z mapping functions offer a robust alternative to existing techniques and are well-suited for a range of digital filter design applications.

References

[1] A. Ouadi, H. Bentarzi and A. Recioui, "Optimal Multiobjective Design of Digital Filters Using Taguchi Optimization Technique" *Journal of Electrical Engineering*, vol. 65, no. 1, pp. 21-29. 2014.

[2] A. G. Radwan, A. M. Soliman and A. S. Elwakil, "First-Order Filters Generalized to the Fractional Domain," *Journal of Circuits, Systems and Computers.* vol. 17, no. 01, pp. 55-66, 2008.

[3] O. P. Goswami, A. Shukla, M. Kumar and A. Bhargava, "Optimal design of digital low-pass filters using multiverse optimization" *Journal of Electrical Engineering*, vol. 75, no. 4, pp. 253-257, 2024.

[4] R. Schaumann and M. E. V. Valkenburg, *Design of analog filters*, Oxford university press. 2001.

[5] A. Antoniou, *Digital Filters: Analysis, Design, and Application.* 2nd edition, McGraw Hill Education. 2001.

[6] D.G. Ćirić, V.D. Pavlović and N.S. Dončov, Generating 2-D FIR filter functions by Christoffel–Darboux formula for Chebyshev polynomials of the second kind. *International Journal of Electronics*, vol.104, no. 3, pp. 416-432, 2017.

[7] F. Leulmi, and Y. Ferdi, Improved digital rational approximation of the operator sα using second-order s-to-z transform and signal modeling. *Circuits Systems and Signal Processing*, vol 34, no.6, pp. 1869-1891, 2014.

[8] D.K. Upadhyay, Class of recursive wideband digital differentiators and integrators. *Radio engineering*, vol. 21, no. 3, pp. 904-910. 2012.

[9] M.A. Al-Alaoui, Linear phase low pass IIR digital differentiators. *IEEE Trans. Signal Process.*,vol. 55, no. 2, pp. 697–706, 2007.

[10] O. P. Goswami, A. Shukla and M. Kumar. "Optimal design and low noise realization of digital differentiator" Journal of Electrical Engineering, vol. 73, no. 5, pp. 332-336, 2022.

[11] M.A. Al-Alaoui, Filling the gap between the bilinear and the backward-difference transforms: an interactive design approach. *International journal of electrical engineering education*, vol. 34, no. 4, pp. 331-337, 1997.

[12] C. Wan and A.M. Schnieder, Further improvements in digitizing continuous-time filters. *IEEE Transactions on Signal Processing*, vol. 45, no. 3, pp. 533 – 542, 1997.

[13] S.K. Mishra, D.K. Upadhyay and M. Gupta, Search of optimal s-to-z mapping function for IIR filter designing without frequency pre-warping. *IETE Journal of Research,* vol. 67, no.6, pp. 853-861, 2021.

[14] S.K. Mishra, D.K. Upadhyay and M. Gupta, Optimized first-order s-to-z mapping function for IIR filter designing, *20th International Conference on Intelligent System Application to Power Systems (ISAP)*, 2020, New Delhi, India. DOI: 10.1109/ISAP48318.2019.9065934.

[15] A.M. Schnieder, J.A. Anuskiewicz and I.S. Barghouti, Accuracy and stability of discrete-time filters generated by higher-order s-to-z mapping functions. *IEEE Trans. Automat. Contr*., vol. 39, no. 2, p. 435–441, 1994.

[16] M.A. Al-Alaoui, Novel stable higher order s-to-z transforms. *IEEE Trans. Circuits Syst. I: Fundam. Theory Appl.,* vol. 48, no. 11, pp. 1326–1329, 2001.

[17] [17] A. Schneider, J. Kanshige and D. Droutage, Higher order s-to-z mapping functions and their application in digitizing continuous-time filters. *Proceedings of the IEEE,* vol. 79, no. 11, pp. 1661 – 1674, 1991.

[18] N.Q. Ngo, “A new approach for the design of wideband digital integrator and differentiator,” *IEEE Transactions on Circuits and Systems II: Express Briefs*, vol. 53, no. 9, pp. 936–940, 2006.

[19] C. Tseng, and S. L. Lee, “Digital IIR integrator design using Richardson extrapolation and fractional delay,” *IEEE Transactions on Circuits and Systems I: Regular Papers*, vol. 55, no.8, pp. 2300–2309, 2008.

[20] C. Tseng, and S. L. Lee, “Digital IIR integrator design using discrete hartley transform interpolation method,” *IEEE Int.Symp. Circuits Syst.*, pp. 2181–2184, 2009. DOI: 10.1109/ISCAS.2009.5118229.

[21] C. Candan, “Digital wideband integrators with matching phase and arbitrarily accurate magnitude response,” *IEEE Transactions on Circuits and Systems II: Express Briefs*, vol. 58, no. 9, pp. 610–614, 2011.

[22] M. Al-Alaoui, “Novel class of digital integrators and differ-rentiators,” *IEEE Transactions on Signal Processing (early access)*, pp. 1–1, 2008.

[23] M. Gupta, M. Jain and B. Kumar, Recursive wideband digital integrator and differentiator. *Int. J. Circuit Theory Appl*., vol. 39, no. 7, pp. 775–782, 2011.

[24] O.P. Goswami, T.K. Rawat and D. K. Upadhyay, A novel approach for the design of optimum IIR differentiators using fractional interpolation. *Circuits Syst. Signal Process.*, vol. 39, pp.1688–1698, 2020.

[25] D.K. Upadhyay and R. K. Singh, Recursive wide band digital differentiators and integrators. *Electron. Lett*., vol. 47, no. 11, pp. 647–648, 2011.

[26] K. Rajasekhar, Fractional Order Differentiators Design Using Honey Badger Optimization Algorithm Based s to z Trans-form. *Wireless Personal Communications,* vol. 139, no. 3, pp. 1565-1591, 2024.

[27] K. Garg and D.K. Upadhyay, Design of second order recursive digital integrators with matching phase and magnitude response. *Radioengineering,* vol. 26, no. 1, p. 376-386, 2017.

[28] M. Jalloul and MA, Al-Alaoui, Design of recursive digital integrators and differentiators using particle swarm optimization. *International Journal of Circuit Theory Application*., vol. 44, pp. 948–967. 2017.

[29] O. P. Goswami, D. K. Upadhyay, and T.K. Rawat, Extended bilinear transform and multirate technique based approach for analog-to-digital transform, *International Journal of Electronics* (Taylor & Francis*), 2021*
Doi: 10.1080/00207217.2021.1969446.

[30] X. Wei, J. Chen, H. Zhao and H. Meng, H, Design of IIR Fractional Order Digital Integrators Using Iterative Convex Optimization Algorithm, *Proceedings of 2024 Chinese Intelligent Systems Conference. Lecture Notes in Electrical Engineering*, vol. 1284. Springer, Singapore.
https://doi.org/10.1007/978-981-97-8654-1_37.

[31] [31] P. Sharan, A.M. Upadhyaya and M.S. Manna, Implementation of digital differentiator and digital integrator using quantum dot cellular automata. *J Opt,* vol. 52, pp.1867–1878, 2023.

[32] M. Massberg, Digital low-pass filter design with analog-matched magnitude response, *Journal of the Audio Engi-neering Society*. 2011.

Received 30 December 2024